Study of the thermomechanical behaviour of a concrete element

Réda Bouabdellah Douhi
Nabila Boualla (bouallanabila2021@gmail.com)
Hamid Khelafi
Tayeb Yahiaoui

Research Article

Keywords: Concrete, Thermal gradient, Fire resistance, Simulation – CASTEM, Mechanical resistance

Posted Date: March 9th, 2022

DOI: https://doi.org/10.21203/rs.3.rs-1424666/v1

Abstract

The need to improve the safety of nuclear reactor containment has revealed the need for data on the thermomechanical behaviour of concrete in the event of an accident during which concrete is exposed to high temperatures. This work aims to study the influence of high temperatures on the behaviour of ordinary concrete specimens charged by a compression force.

A thermal model is developed by a volumetric discretization (CASTEM). The results of various simulations, combined with other findings, allow a physical explanation of the thermomechanical phenomenon of concrete structures, which made it possible to obtain the variation of the stresses in any point or node and for each temperature in different directions X, Y and Z.

Introduction

Concrete is a material that performs well when subjected to high temperatures. This is one of the reasons why it is widely used for the construction of supporting structures of buildings and civil engineering works. But despite this good behaviour, in the face of a fire, the performance of the material can be more or less affected. Analysis of the fire resistance of reinforced concrete structures is an important part of their design. In the analysis, an engineer typically uses various formulas for the fire resistance of structures offered by building codes, without really understanding the thermo-mechanical behaviour of a structure during a fire (Bratina et al., 2005).

Research on thermo-mechanical behaviour and material functionally graded material design has attracted considerable attention in recent years, particularly in structural ceramic applications (Awaji and Sivakumar, 2001; Choudhury et al., 2014; Wang et al., 2015). They found that the damage behaviour is generally associated with the cooking temperature in both concrete (Kakroudi et al., 2008). High temperatures are described as one of the most critical physical damage procedures that affect the quality and strength of concrete structures (Baghdadi et al., 2021; Belgacem et al., 2021). A functionally graded material is a type of composite material whose physical and mechanical properties vary spatially along with certain directions to obtain specific thermal and/or mechanical properties for specific applications (Wang et al., 2015). Therefore, by analyzing the thermo-mechanical behaviour of such materials, simulations under operating conditions offer a great practical contribution (Bareiro et al., 2021).

This work aims to develop a finite element model for the analysis of concrete structures under combined thermal and mechanical loads, to benefit from a fast and efficient time and cost point of view in the optimization of real prototypes.

Temperature rise during cement hydration remains an open problem in mass construction concrete works. Due to the considerable thickness of these structures, the amount of heat generated is important and the core of the concrete element reaches particularly high temperatures, which is also higher than the temperature of its surface layers. Such a non-uniform temperature distribution and its variation over time induce thermal stresses (Klemczak et al., 2018).

To verify the capacity of the model, the simulation results are compared with the experimental results. We used a test piece with a simple geometry in the form of a three-dimensional (3D) cubic parallelepiped. A series of test validation of different temperature levels (25°C to 500°C) is carried out to treat the influence of temperature on the mechanical behaviour of the specimen. The measurement parameters used are Temperatures and stresses.

Most mechanical studies of high-temperature concrete deal with the behaviour of the material in uniaxial compression. This is explained by the relative simplicity of the required experimental techniques and by the fact that the compressive strength of the concrete contributes to the overall stability of the structures (as opposed to tensile strength) (Phan, 2003). The results for a compression load of 65 MPa are presented.

Materials And Methods

Most of the mechanical studies of high-temperature concrete relate to the behaviour of the material in uniaxial compression. This is explained by the relative simplicity of the required experimental techniques and the fact that the resistance to concrete compression contributes to the overall stability of the structures (in contrast to tensile strength).

The aim is to develop a finite element model for the analysis of combined thermal and mechanical concrete structures on a compression-loaded concrete test piece. The objective of this is to perform and analyze numerical simulations on different concrete. The numerical implementation of the thermal aspects of concrete is quite complex (Douk et al., 2021).To do this, we used the CASTEM 2000 Software, developed by the Department of Mechanics and Technology (DMT) of the French Commissariat à l'Energie Atomique (CEA). This calculation code is based on the analysis of structures by the finite element method.

We used a simple geometry in the form of a three-dimensional cubic block (three-dimensional (3D)) with an eight-node quadratic mesh (Fig. 1).

In order not to overload the calculations, we linked the entire specimen and simplified the geometry of the element. The mesh is densified partly exposed to fire, where the thermal gradients are the most important. The elements used are elements of type CUB8, hexahedron at 8 knots. The average size of the elements is (7x7x7) cm^3 and the mesh geometry has 340 elements (Fig. 1).

Results And Discussion

Mechanical boundary conditions specific to CASTEM make it possible to account for the symmetry of the structure. These conditions are applied to the planes of symmetry of the structure (a three-dimensional (3D) plane). The test piece rests only on its base S1. The vertical and horizontal displacements of this zone are blocked while avoiding the rotation to create a local embedment which would result in a

concentration of stresses too large and realistic at the point located on the planes of symmetry. When the heater reaches the ISO 834 curve of Eurocode 2 (1991, 2002) the mechanical load is applied.

The initial thermal condition is to apply a temperature of 25°C to the entire volume, exposing the surfaces (S2 S3 S4 S5 and S6) to the fire.

The interest of this modelling lies in the effect of determining the actual stress at the compression of concrete subjected to a thermal charge, by knowing the stress of the same concrete which has undergone mechanical loading tests in the laboratory after cooling the test pieces and thus avoiding the additional stress of the tests.

The evolution of the stress difference was visualized on origin 8 in 100 points giving a constant step, allowing us to model its pace with an approximation of the order of (ε = 0.99602). The variation of stresses (Y) or differences in stresses is given by a polynomial function of order 2: T = 2.34861 + 0.12659 * T + 1.3245E-4 * T2.

Figure 2 represents the contour of the calculated temperatures of the thermomechanical simulation, considering that the behaviour of the material (concrete) is linear elastic. thermomechanical behaviour concretes has been strongly influenced by the nature and adhesion of aggregates (Boussuge, 2008). It is observed that the temperature rises very quickly in part exposed to the heat flux while the unexposed part does not show very important heating.

This figure thus highlights the important thermal gradients which occur in the thickness of the test piece. This can be explained by the thermal stress and low thermal diffusivity of the material. We find that the influence of heat flux temperature is noticeably apparent on the specimen (Fig. 3). The latter lose their mechanical performance in the temperature range of [25°C, 200°C] (phase I) and then resumes after this threshold, a partially weak growth with a significant peak in the vicinity of 400°C (phase II) then it loses their performance and falls completely (Phase III).

Figure 3c shows the direction of heat flow inside the cube, it obeys the natural phenomenon of heat propagation that moves from high-temperature areas to low-temperature areas by conduction.

Here we present the results of the thermomechanical simulations carried out considering that the behaviour of the studied material (ordinary concrete) is linear elastic.

In Fig. 4, we have shown the temperature contour of the thermomechanical simulation. It should be noted that the temperature rises very quickly in part exposed to the heat flux while the unexposed part does not show very significant heating.

In the next paragraph, we treat the measured resistances under thermal loading (Fig. 5). All authors agree that the compressive strength of (ordinary) concrete varies with the temperature at which it is exposed. It decreases overall with the temperature rise. The analysis of the evolution curve (Fig. 5) of the heat resistance as a function of temperature allows us to group this evolution in the following phases:

We find that the influence of heat flux temperature is noticeably apparent on the specimen. The latter loses its mechanical performance in the temperature range of [25°C, 200°C] (phase I). In the interval [100°C, 200°C], the tests show a decrease in compression resistance. To this must be added the increase in microfissuration and porosity, the influence of the nature of the paste and the aggregates and the differential deformations between the paste and the aggregates (Khoury, 2008).

The thermal expansion of solids is expressed as the fractional increase in the length of a material per unit increases in temperature (Malik et al., 2021). Under the impact of thermal actions, temperatures increase, this phenomenon is called «thermal transfer». The latter potentially leads to thermal expansion and deterioration of mechanical properties in heated parts. The latter can result in the spacing of the sheets of the C-S-H gel. This spacing generates a reduction of the cohesion forces of the Van der Waals type between the sheets (Ožbolt et al., 2009). The thermal expansion of concrete is conditioned by the thermal expansion of two phases: the thermal expansion of cement paste and the thermal expansion of aggregates. In addition, hardened cement paste and aggregates have two very different thermal behaviours: from 150°C, the paste contracts while the aggregates continue to swell. This difference in behaviour is all the more important as the aggregates show a high thermal expansion, as can be the case with aggregates with high silica content. We are therefore in the presence of a deformation incompatibility that causes tangential stresses at the cement paste/aggregate interface (Phan, 2007)0

Between [250°C, 300°C] (see 400°C) (Phase II). Partially weak growth with large peaks. In the bibliography, this increase is explained by the low permeability of the concrete. The departure of the water is therefore slowed down. Chemical decomposition and associated water loss cause significant changes in the microstructure of cement pastes. According to the departure of the water leads to rehydration of the dough due to the migration of the water into the pores (Bažant and Kaplan, 1996).

In the [350°C, 400°C] domain, microcracking can occur as a result of incompatibility between the thermal expansion coefficients of cement paste and aggregates. Beyond 400 the test piece completely loses its performance (phase III). The drop in resistance is due to the development of micro-fissures caused by the difference in coefficients of thermal expansion of the components and by the decomposition of calcium hydroxide. In the literature, all authors find this drop in resistance in the field beyond 350°C.

Due to mechanical loading, the specimen is deformed. Following the two Ox axes, a deformation of the specimen was caused by the stresses imposed along the Oz axis (Fig. 7,8).

The experimental curve shows a temperature difference. The fact of considering that the characteristics of the material are constant about the temperature does not accurately reflect what happens in the concrete during heating.

Unlike the mechanical loading phase, heating causes stresses to develop along the Ox and Oz axis (Oy and Oz respectively) which are very close to each other. The evolution of the stresses at several depths of the specimen (Fig. 9,10,11) clearly shows the sign of the appearance of a double curvature according to

these two planes. This aspect of thermomechanical behaviour is accessible to us only thanks to the three-dimensional (3D) framework of the modelling.

It is noted that the intensity of the heat flux temperature stresses fixed at 400C°, the maximum stress is in the region of the core because this place undergoes the greatest stress, and it is less important at the level of the embedment, because of the limits imposed (Fig. 9,10,).

To do this, we drew the profile of the stresses generated along with the centre thickness and the first centimetres of the test piece along the Ox axis of the core projected on the S5 surface and the Oy axis projected on the S6 surface (Fig. 9). In the elastic range, the 3 components reach their maximum values at the same time for a temperature close to 400°C. The stress along the Oz axis is the most important. It governs the behaviour of the test piece, which explains the mode of rupture observed on the test pieces.

We note at first that the constraints developing along the Ox and Oy axis are less important compared to the constraints along the Oz axis. This is representative of the fact that the test piece is simply supported on its S1 base from its sides, thus favouring a main bending plane (Oz).

Figures 11 and 12, Stress σz as a function of the depth of the next cube We note at first that the constraints developing along the Ox and Oy axis are less important compared to the constraints along the Oz axis. This is representative of the fact that the test piece is simply supported on its S1 base from its sides, thus favouring a main bending plane (Oz).

In addition, the re-increase in strength that accompanies the temperature rise after 400°C is attributed to the stiffening of the cement paste microstructure due to the departure of adsorbed water. It is accepted that the presence of water between two gel walls attenuates the surface forces (Van der Waals forces) between the gel particles, and thus reduces the strength of the concrete. The departure of adsorbed water causes the increase of surface forces between the gel particles, resulting in a rise in the strength of the concrete.

Between 400 and 500°C, we see a rapid deterioration in the mechanical properties of concrete. CASTILLO et al attribute this to the acceptance that cracks in a mechanically loaded test piece are not free to develop. This delays degradation due to differences in the coefficients of thermal expansion of components.

The decrease in strength can be attributed to a structural change of the concrete, as a result of differences in the coefficients of thermal expansion of the different components. We have a clear increase in porosity and microfissurations of the material. Concrete degradation may also be related to the decomposition of $Ca(OH)_2$.

Constraints σx and σy are less important than σz (σz > σx of 30%) (Fig. 13). This is representative of the fact that the test piece is simply supported on its S1 base, thus favouring a main bending plane (Oz).

The results shown in Fig. 14 are presented as iso-colours. These figures show the temperature intensity set at 400 C°. There is a clear difference in stress from the outside to the inside of the block studied. The stress reaches its maximum value in the region of the core of reason that this place undergoes the greatest stress, and, less important at the level of embedment, due to the limits conditions imposed previously.

The stress reaches its maximum in which part in the region in the position shown below The constraints σx and σy is less important than that of σz (σz > σx of 30%) (Fig. 15). This is representative of the fact that the specimen is simply supported on its S1 base from its sides, thus favouring a main bending plane (Oz).

Figure 15 shows the evolution of the calculated displacements at the centre of the test piece (P0) and one of the angles of the test piece (node) (P1, P2, P3, P4, P5, P6, P7, P8). From the first seconds of heating, a bi-axial compression state is observed at the part exposed to fire, where the displacement develops very significantly.

The stresses are bounded by the resistance of the material in compression. As a result, the Oz-axis constraints appear to govern the behaviour of the specimen.

For this purpose, we observed the temperature field at the precise location where the scales of heat transfer were located when heating surfaces were exposed to fire. It has been found that the evolution of the surface temperature Tpx, Tpy and Tpz simulated or recorded at any distance along the Ox, Oy and Oz axes of the fire surface is proportional to the growth of the heat flux. (Fig. 16).

We observe the same gaits for all the figures that explain the drop in temperature, from the exposed surface to the cube core through different zones for each experiment (T = 100, 200, 300, 390,400 and 500°C) (Fig. 17), each figure gives us the distribution of the temperature inside the cube. The speed of each curve is similar for all experiments with a decay of the temperature from outside to the core. This temperature gradient between the outer part of the cube and its core is different for each experiment due to the influence of temperature on the main parameters of the material such as conductivity.

The cubic specimen subjected to a flow of heat from the outside causes the temperature to propagate to the core in an inverse way to the exponential.

Conclusion

Exposing concrete to high temperatures, such as in a fire, causes physical and chemical changes that can lead to deterioration of mechanical properties, cracking and spalling. Exposing concrete to high temperatures, such as in a fire, causes physical and chemical changes that can lead to deterioration of mechanical properties, cracking and spalling (Fernandes et al., 2017). During a fire, the microstructure of concrete undergoes major physical-chemical changes that influence its mechanical behaviour. The present study has a numerical character using the CASTEM calculation code, and has enabled us to

study the thermomechanical behaviour of concrete in the field of heat transfer under mechanical stress, from this study we can conclude that: experimental model despite its indispensable.

Increasing the thermal diffusivity of concrete would minimize the thermal gradients that increase in concrete during heating.

The results seem motivating, which shows good agreement with the experimental results found in the literature.

Note that our resistances have been determined after cooling; the concrete is a little damaged during cooling. The drop in resistance is therefore mainly due to the increased thermal stress.

The temperature engendering all-around a structure can influence the mechanical characteristics of the structure, among these characteristics is the Young module.

From T = 400°C, the structure can withstand compression, which demonstrates a peak validated by that of the experimental.

From this simulation, we can detect in any zone in the structure (cube) the temperature, the deformation and the stress without systematically making use of the experimental model despite its indispensable.

Increasing the thermal diffusivity of concrete would minimize the thermal gradients that increase in concrete during heating.

References

1. G.A. Khoury. Polypropylene fibres in heated concrete. part 2: pressure relief mechanisms and modelling criteria. Magazine of concrete research, 60(3) :189–204, 2008.
2. J. Ožbolt, G. Periškić, M. Jelčic, and H.W. Reinhardt. Modelling of concrete exposed to high temperature. In 1st International Workshop on concrete spalling due to Fire Exposure, pages 461–469, Leipzig, 2009.
3. L. T. Phan. Spalling and mechanical properties of high strength concrete at high temperature. In Consec'07, 1595–1608, Tours, France, 2007.
4. U. Schneider, U. Diederichs, and C. Ehm. Effect of temperature on steel and concrete for PCRVŚ. Nuclear Engineering and Design, 67:245–258, 1987.
5. Z.P. Bažant and M.F. Kaplan. Concrete at high temperatures: material properties and mathematical models. Longman, longman group limited edition, 1996.
6. Code de calcul par éléments finis CASTEM. Commissariat à l'Energie Atomique CEA-DEN/DM2S/SEMT. Complex Effect of Concrete Composition on the
7. B. Klemczak, M. Batog, Z. Giergiczny, A. Z˙mij. Complex effect of concrete composition on the thermo-mechanical behaviour of mass concrete.. Materials, 11(11), 2207, 2018.

8. W. Zhou, C. Feng, X. Liu, S. Liu, C. Zhang, W. Yuan, Contrastive Numerical Investigations on Thermo-Structural Behaviour s in Mass Concrete with Various Cements. Materials 2016, 9, 1–19.
9. H. Awaji, R. Sivakumar. Temperature and stress distributions in a hollow cylinder of functionally graded material: the case of temperature-independent material properties. Journal of the American Ceramic Society 84(5): 1059–1065, 2001.
10. A. Choudhury, S.C. Mondol, S. Sarkar. Finite element analysis of thermo mechanical stresses of two layered composite cylindrical. International Journal for Research in Applied Science & Engineering Technology 2(XI): 341–349. 2014.
11. Z.W. Wang, Q. Zhang, L.Z. Xia, J.T. Wu, P.Q. Liu. Stress analysis and parameter optimization of an FGM pressure vessel subjected to thermo-mechanical loadings. Procedia Engineering 130: 374–389. 2015.
12. W.G. Bareiro, E.D. Sotelino, F. de Andrade Silva. Numerical modelling of the thermo-mechanical behaviour of refractory concrete lining. Magazine of Concrete Research 73(20): 1048–1059. 2021. https://doi.org/10.1680/jmacr.19.00371.
13. Eurocode 2. Design of Concrete Structures, Part 1: General rules and rules for buildings, ENV 1992-1-1, 1991.
14. Eurocode 2. Design of Concrete Structures, Part 1–2: General rules–Structural Fire Design, prEN 1992-1-2, 2002.
15. S. Bratina, B. Čas, M. Saje, I. Planinc. Numerical modelling of behaviour of reinforced concrete columns in fire and comparison with Eurocode 2. International Journal of Solids and Structures. 42 (21–22), 5715–5733, 2005.
16. M. Boussuge. Investigation of the thermomechanical properties of industrial refractories: the French programme PROMETHEREF. Journal of Materials Science, 43(12), 4069–4078. 2008. doi: 10.1007/s10853-008-2534-0.
17. Kakroudi M.G., Yeugo-Fogaing E., Gault C., Huger, M., Chotard T. (2008): Effect of thermal treatment on damage mechanical behaviour of refractory castables: Comparison between bauxite and andalusite aggregates. Journal of the European Ceramic Society, 28(13), 2471–2478. doi: 10. 1016/j.jeurceramsoc.2008.03.048.
18. Baghdadi M., Dimia S.M., Guenfoud M., Bouchair A. (2021): An experimental and numerical analysis of concrete walls exposed to fire. Structural Engineering and Mechanics, 77(1), 819–830. doi: 10.12989/sem.2021.77.6.819.
19. B. Mamen, F. Benali, A. Boutrid, M. Sahli, M. Hamidouche, G. Fantozzi. Experimental investigation and non-local modelling of the thermomechanical behaviour of refractory concrete Ceramics-Silikáty 65 (3), 295–304. 2021.
20. N. Douk, X. Hong Vu, A. Si Larbi, M. Audebert, R. Chatelin. Numerical study of thermomechanical behaviour of reinforced 2 concrete beams with and without textile reinforced concrete (TRC) 3 strengthening: effects of TRC thickness and thermal loading rate 4. Engineering Structures, 231, 111737. 2021.

21. B. Fernandes, A.M. Gil, F.L. Bolina, B.F. Tutikian, Microstructure of concrete subjected to elevated temperatures: physico-chemical changes and analysis techniques. Revista IBRACON de Estruturas e Materiais, 10, 838–863. 2017.
22. M. Malik, S.K. Bhattacharyya, S.V. Barai, Microstructural changes in concrete: Postfire scenario. Journal of Materials in Civil Engineering, 33(2), 04020462. 2021.

Figures

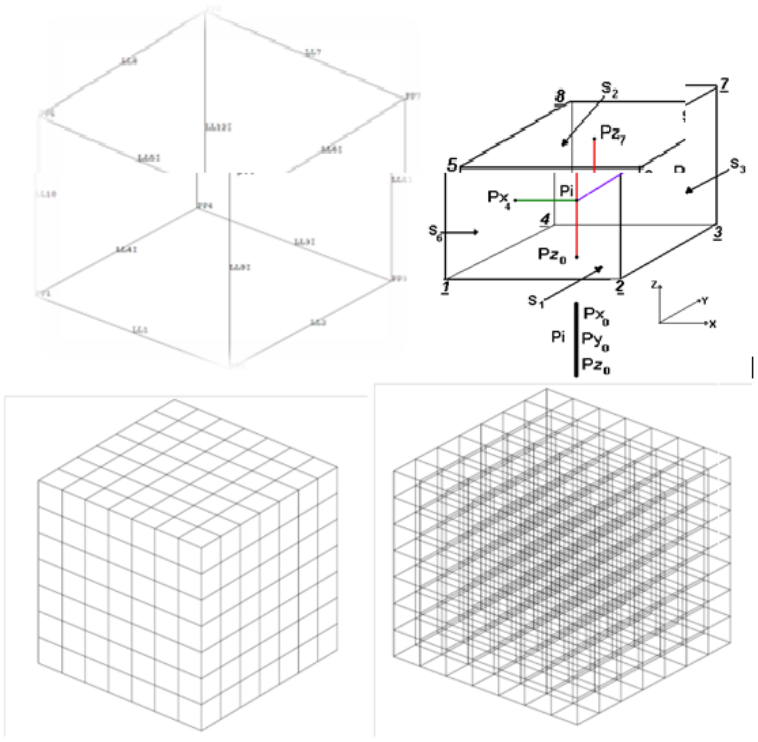

Figure 1

The geometry of the test piece

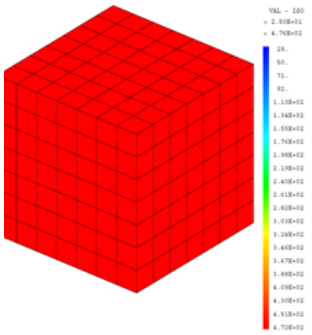

Figure 2

Thermal gradient distribution

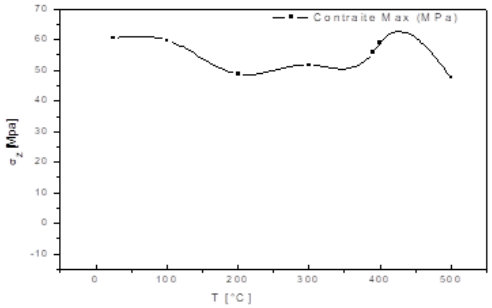

Figure 3

Influence of heat flux temperature on stress σz

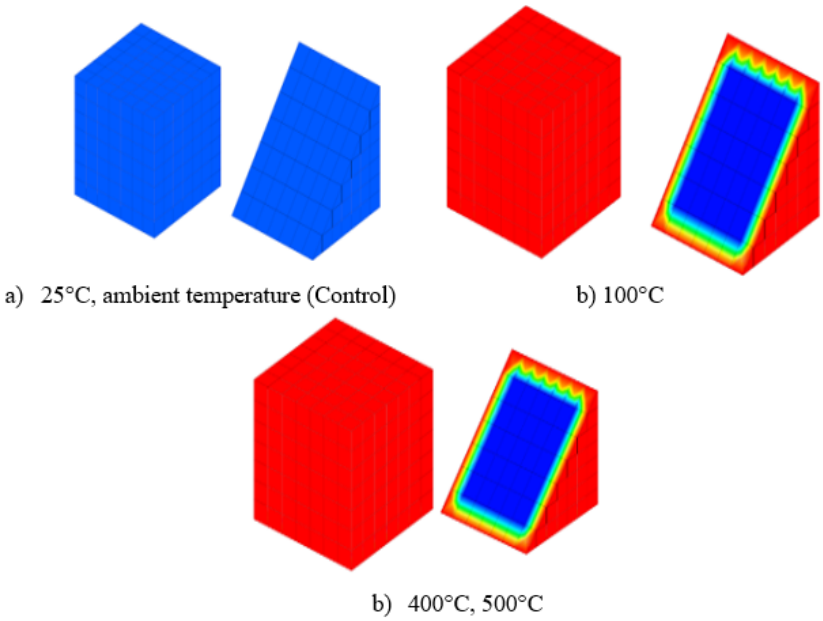

Figure 4

Distribution of thermal gradients in the test piece

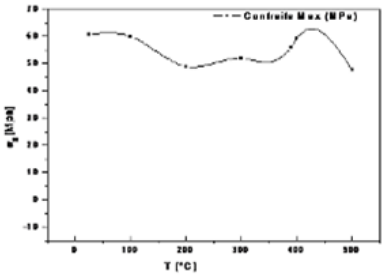

Figure 5

Influence of heat flux temperature on stress σz

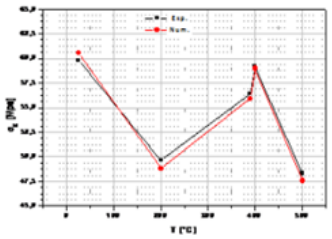

Figure 6

Stress as a function of temperature

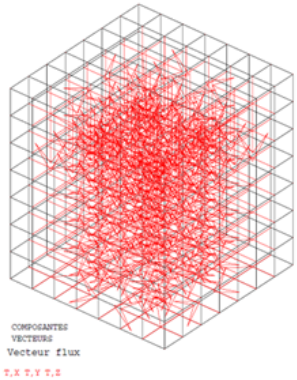

Figure 7

Propagation of the Heat Flux in the Cube

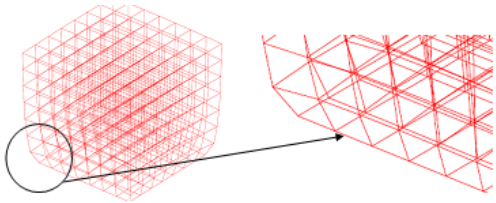

Figure 8

Image of the deformation with a zoom in the most deformed area

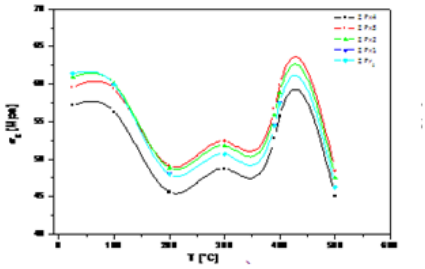

Figure 9

Stress σx concerning heat flux temperature

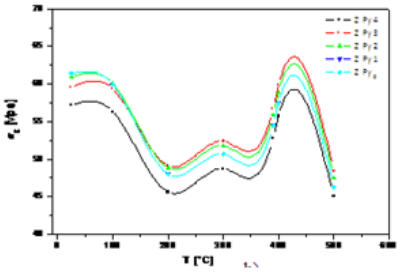

Figure 10

Stress σz with heat flux temperature

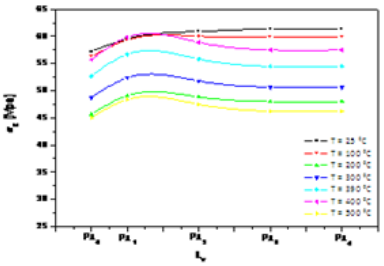

Figure 11

Stress σz as a function of the depth of the next cube

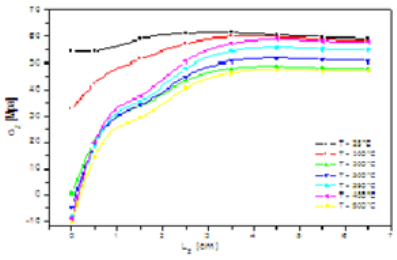

Figure 12

Stress σz as a function of the depth of the cube along the Oz axis

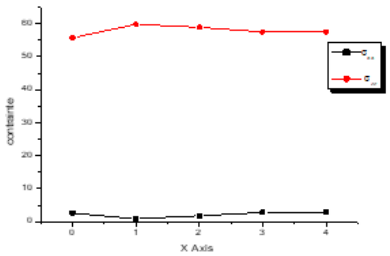

Figure 13

Stress comparison σz and σx

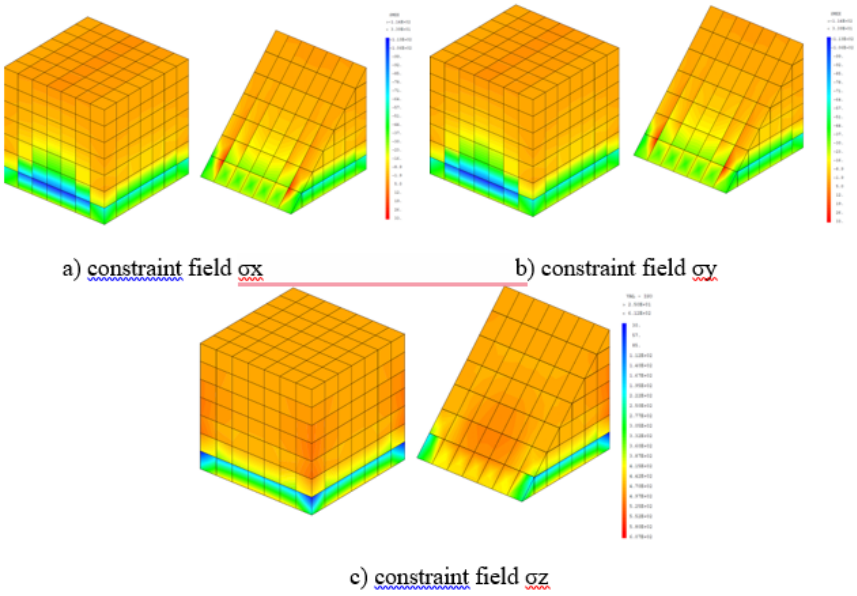

Figure 14

Stress field mapping

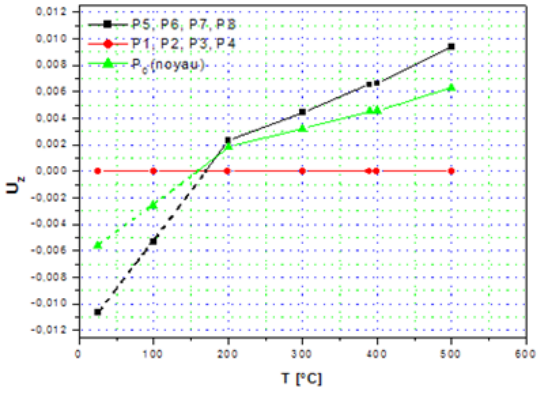

Figure 15

Displacement of the nodes calculated according to the imposed temperatures

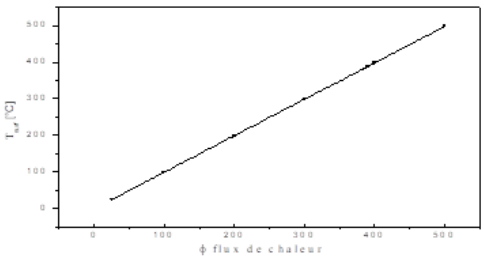

Figure 16

Evolution of surface temperature as a function of heat flow

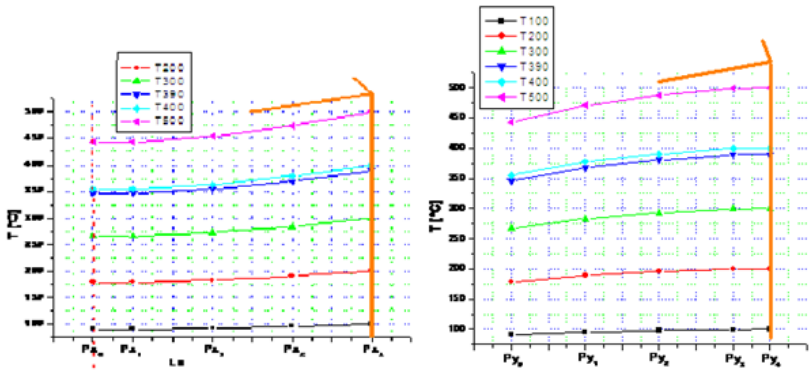

Figure 17

Evolution of temperature propagation to the core for various surface temperatures imposed